İSTANBUL UNIVERSITY CERRAHPAŞA

ORIGINAL ARTICLE
Electrica 2022; 22(2): 258-266

CBMIR System Based on Matrix Weighting Framework and Linear Transformation with KNN

Shahin Shafei[1], Hamid Vahdati[1], Tohid Sedghi[2,3], Asghar Charmin[1]

[1]Department of Electrical Engineering, Ahar Branch, Islamic Azad University, Ahar, Iran
[2]Department of Electrical Engineering, Urmia Branch, Islamic Azad University, Urmia, Iran
[3]Microwave and Antenna Research center, Urmia Branch, Islamic Azad University, Urmia, Iran

Cite this article as: S. Shafei, H. Vahdati, T. Sedghi and A. Charmin, "CBMIR system based on matrix weighting framework and linear transformation with KNN," *Electrica.*, 22(2), 258-266, 2022.

ABSTRACT

Biomedical images are utilized by radiologists and physicians in cases where diagnosis and recognition would be more efficient. Therefore, it is recommended to propose novel methods that can retrieve medical images with a high percentage of accuracy. A comprehensive feature selection and weighting combination method with novel learning of k-nearest neighbor artificial neural network (KNN-ANN) was introduced for retrieval of biomedical MR images. Modified Radon, and modified Hu moments operators with weighting combinational methods were proposed for achieving a higher percentage of retrieval. Moreover, these characteristics are re-composed for presenting outstanding statistic specification and spatial signals. This spatial and frequency information is obtained for all MR image datasets. The composition of shape and textural features presents robust vectors for retrieval of the biomedical database. In addition, a KNN-ANN framework is proposed and applied to measure the similarity between the query and biomedical database. The presented system achieves 90% retrieval for all types of classes. For matching features, the most similar highest priority principle with KNN is used. The image retrieved from the databases is the image which has less distance and less most-similar highest priority at KNN. The proposed algorithm is evaluated on two different databases. This novel scheme illustrates higher and better specialty in the MRI datasets. The results were compared and understood to be remarkable.

***Index Terms*—**artificial neural networks, feature generation, retrieval, recall.

I. INTRODUCTION

The main problem in content-based medical image retrieval (CBMIR) systems for MR images is the gap between the low-level data produced by the MRI systems and the high-level data understood by the operator [1-3]. The old feature extraction techniques work on low-level features to decrease the distance of the gap. Deep learning techniques are strong for feature generation that can show data entirely and set the level of feature production at self-learning. The oldest method of medical CBMIR utilizes labels, or keywords, to refer to biomedical images in way that they can be retrieved based on feature descriptors. Manual labeling systems are laborious and time-consuming [4,5]. Shape-based medical image retrieval (SBMIR) systems illustrate the retrieval of medical images from the datasets on the basis of syntactical image features. The features utilized consist of shape, texture, and multiresolution transformations like Gabor, simple wavelets, or multiscale filtering [6]. Section-to-section similarity between the images of a dataset are evaluated in [6,7], but these methods are outdated. In [8], the matching of integrated sections illustrates the similarity of all regions. Each part of a region is given superiority based on the evaluation of its window size. In [9], fuzzy features are utilized to achieve the biomedical image descriptors. Shape features are generated from biomedical images, and some moments are utilized for shape attributes. Their retrieval performance is premium, compared to other integrated region systems like [9,10]. To screen incoherent biomedical images of a dataset, the preprocessing and classification are used in the first level of the system. Previous researches depict that combined generated features affect the characteristics of the similarity between biomedical images. Besides, these methods use the partitioning principle, which is not useful in shape specification. Search in spatial and local data of combined features is used in target-based retrieval, which is superior compared to partitioning methods [11,12]. The biomedical images are segmented into different regions based on the texture and color features, in region-based

Corresponding author:
Tohid Sedghi
E-mail: sedghi.tohid@gmail.com; t.sedghi@iaurmia.ac.ir

Received: October 20, 2021

Revised: December 24, 2021

Accepted: January 3, 2022

DOI: 10.54614/electrica.2022.210130

medical image retrieval (RBMIR) systems [13,14]. The segmentations are close to human perception. They are utilized as the first platform blocks for similarity analysis and feature calculation. The old indexing methods are inferior when compared to the RBMIR systems, which have been proven to be outstanding. The individual region-to-region similarity check is studied in [15]. These systems have a weakness in that they are time-consuming. Therefore, different image segmentation methods have been an open area of research in recent times [16]. The integrated segmentation matching (ISM) system is introduced in [16]. In this method, an image similarity check based on merging all regions is presented. Each section is assigned a value of its importance, based on the size of the biomedical image. In addition, fuzzy features are used to capture the shape information. Shape features are calculated based on spatial information, and the invariant modified moments are then utilized as the shape specifications. The retrieval characteristic of [16] has been proven to be smarter than different previous systems such as [5-9]. The studies indicated above obviously present that, in CBMIR, spatial information with local features has a great role in specifying the medical image similarity. It is difficult to obtain shape determination at object detection using segmentation methods. A special windowed search over scale and location is proven to be more efficient at object-based medical image retrieval (OBMIR) than the algorithms based on segmentation in [16]. The present research is proposed to present a novel method to use improved Radon transform (R-transform) with weighting composition in a deep learning frame of ANN. Improved Hu operators are computed as shape descriptors, Also, a deep learning framework is utilized for retrieval. The deep learning with the composition of features forms remarkable feature-vectors in the retrieval process. Deep learning and the weighted matrix method are used to improve the retrieval performance. The study is done with a total of 3063 MR image datasets that contain three types of brain tumors (introduced in three different classes). For better comparison of the results, a second database with 9000 MR images is introduced. The presented system has minimum preprocessing and is less time-consuming, can obtain a mean average 90% retrieval, and performs better on the CBMIR on the MR image databases. All previous methods are complex because of the need to use different kinds of algorithms which involve maximum processing. The results are compared with different algorithms in two databases.

II. WEIGHTING OF R-TRANSFORM & HU BASED FEATURES

A. Generation of Textural Feature Dataset on R-Transform

A biomedical image of a database can be shown by various types of projections chosen at various angles. Biomedical image analysis shows a binary planar shape for shape analysis. Thus, for improving the R-transform, it is better to consider a method in which the R-transform function is substituted by a special form of function with $s_D(x,y)$:

$$s_D(x,y)=\begin{cases}1, & if\,(x,y)\in D\\ 0 & otherwise\end{cases}. \tag{1}$$

The R-transform explains the intersection number of all the lines of intensity with the above function. R-transform achieves a rectangular array of cells. R-transform is variant to transformations, and therefore cannot present the shape features. In addition, one-dimensional information is produced from every section ordered row-to-row and column-to-column. The energy (E) and standard deviation (б) are calculated on one-dimensional signals of R-transform. These parameter values are joined to form the initial feature vector. The utilization of energy as a textural feature is due to the fact that this parameter indicates the textural data of a biomedical image. The feature vectors extracted from the regions are expressed as:

$$\overline{f_j}=[E_{11_j},...,E_{1N_j};E_{21_j},...,E_{2N_j};\quad \sigma_{11_j},...,\sigma_{1N_j};\sigma_{21_j},...,\sigma_{2N_j}]$$

$$=[f_{1_j},f_{2_j},...,f_{4N_j}]^T;\ j=1,2,\&\ 9; \tag{2}$$

where Ein_i, *I for* 1,2 *n for* 1,2,...,*N,* and σ_{in_j}, $i=1, 2, n=1, 2, ..., N, j=1, 2, \ldots, 9$, $N=$the number of sections, $j=$the number of partitions, $Ein_j=$the R-transform amplitude norm-1 parameter of energy, $\sigma_{in_j}=$Deviation of standard calculated at the *n*th section for the *j*th signals:

$$E_{norm1}=\frac{1}{Q}\sum_{\alpha\&f\in D}\left|S_x^{\alpha}(f)\right| \tag{3}$$

$$\sigma=(\frac{1}{Q}\sum(S_x^{\alpha}(f)-\overline{S}_x^{\alpha}(f))^2)^{1/2} \tag{4}$$

In addition, R-transform can reduce the noise ratio, with better results than old filters such as the wavelet transform and spectral coloration function. The main signal connecting to the R-transform is analyzed, that is, the mother R-transform signal is amplified. The generated features of the R-transform are utilized to study the textural descriptors. The improved function of R-transform is utilized to increase the frequency data of a biomedical image at a very low resolution and lower the frequency data of the biomedical image at a high resolution. Therefore, for extracting textural descriptors, coefficients are assigned to every signal section.

Weighting of texture and shape descriptors makes a dataset of features:

1. Discrete improved-function R-transform.
2. Enhanced fast-calculated Hu moments

Traditional Hu moments calculations are slower when compared to R-transform. Moreover, R-transform can generate different sub-bands for different orientations. In addition, the R-transform allows decreasing terms, which benefits the shift invariance property. The R-transform is depicted in a symmetric shape between different multi-resolution transforms. The biomedical images of the database are separated into different sub-bands utilizing the R-transformer.

The σ_l (standard deviation) and E_l (energy) are calculated for every sub-band of R-transform. At different biomedical image sub-bands, the standard deviation and energy are achieved as:

$$\sigma_I=\sqrt{\frac{1}{MN}\sum_{k=1}^{M}\sum_{j=1}^{N}\left|M_I(k.j)-\mu_I\right|^2}\quad,\quad E_I=\frac{1}{MN}\sum_{k=1}^{M}\sum_{j=1}^{N}\left|M_I(k.j)\right|^2 \tag{5}$$

The sub-band of R-transform is M_l(i,j), and the window dimension of every sub-band is $M \times N$. The mean value of the sub-band frequency is μ_j. The dataset of the main weighted features is produced by the

sub-bands of R-transform data. A database of biomedical image features is obtained by σ and E of different sub-bands:

$$\bar{f}^k_{\sigma E} = [\sigma^k_1, \sigma^k_2, ..., \sigma^k_L, E^k_1, E^k_2, ..., E^k_L] \quad (6)$$

The generated feature size is 2L in the first level.

B. Shape Features Extraction

Hu is a set of non-linear moments, invariant to orientation and translation property. A set of six moment invariants is deemed to be adequate for all applications. The higher-order moments have deduced to higher sensitivity. All the moments are normalized to introduce central moments. The geometrical moment is computed as:

$$m_{pq} = \sum_{x=0}^{M-1}\sum_{y=0}^{N-1} x^p y^q f(x,y) \quad (7)$$

Image function is $f(x, y)$.

Geometrical central moments can be calculated as:

$$\mu_{pq} = \sum_{x=0}^{M-1}\sum_{y=0}^{N-1} (x-\bar{x})^p (y-\bar{y})^q f(x,y) \quad (8)$$

$\bar{x}$ and $\bar{y}$ are image gravity center and are computed as:

$$\bar{x} = \frac{m_{10}}{m_{00}}, \qquad \bar{y} = \frac{m_{01}}{m_{00}} \quad (9)$$

The number of foreground pixels is $m_{00} = \mu_{00}$. This parameter has no major relation to scale, so central Hu moments can be normalized in scale with (10):

$$\eta_{pq} = \frac{\mu_{pq}}{m^a_{00}} \quad , \quad a = \frac{p+q}{2} + 1 \quad (10)$$

$$\begin{aligned} \phi_1 &= \eta_{20} + \eta_{02} \\ \phi_2 &= (\eta_{20} - \eta_{02})^2 + 4\eta^2_{11} \\ \phi_3 &= (\eta_{30} - 3\eta_{12}) + (3\eta_{21} - \eta_{03})^2 \\ \phi_4 &= (\eta_{30} + \eta_{12})^2 + (\eta_{21} + \eta_{03})^2 \end{aligned} \quad (11)$$

$$Combined\ Feature\ Vectore = [I_{fv}; HueFeatureVectore]$$

After computing Hu, the values will be inserted into the previous vectors. For extracting optimum features, principal component analysis (PCA) is a popular algorithm to reduce features based on Eigen vectors. Hence, only PCA algorithms are applied to the combined feature vector.

$$Combined \quad Feature \quad Vectore = [I_{fv}; HueFeatureVectore] \quad (12)$$

III. K-NEAREST NEIGHBOR ARTIFICIAL NEURAL NETWORK TRAINING PROCEDURE

When a single type of feature is generated from the biomedical image, a large amount of information is lost. Therefore, a combination of extracted features is presented to enhance the accuracy of retrieval. Moreover, weighting of feature recombination produces robust features. Using the weighting feature procedure, the combination produces good retrieval accuracy compared with [1] and [6]. This paper proposes CBMIR for retrieval of similar biomedical images. For achieving better features and for the ultimate performance of the system, the VGG19 neural network model is used in addition to the high-level features. The k-nearest neighbor artificial neural network (KNN-ANN) model is used to meter the similarity among the generated features of the biomedical image database and the query. The features extracted from VGG19 are inserted into KNN-ANN. The features generated from the VGG19 upper levels provide good consequence, since the upper levels in the VGG19 are conveyed to the special features of the biomedical image learned layers. This learning method is presented in [7], in which the multilayer perceptron (MLP)-ANN was utilized as a feature generator. The MLP-ANN learning method is set out from the first input level to the ultimate layer in a back–forward mode. After that, error back propagation is set out from the final level towards the first level. All weights in the MLP-ANN in the levels are computed in the form of linear learning. The last level utilizes the rectangular window feature table and captures the average value of the square window. For data compression, the algorithm reduces the feature table size. The ultimate layer calculates the retrieval expectancy of every class type for detecting the type of image. Unknown weights of KNN-ANN are learned, with the back propagation method. For minimizing the cost function, the gradient descent algorithm is applied over the KNN MLP.

IV. EVALUATION RESULTS IN THE EXPERIMENTAL FRAMEWORK

This section evaluates the efficiency of the proposed system, in comparison to those previously presented by scholars in the literature. The MR image databases at (www.figshare.com/articles/brain_tumor_dataset/1512427) are used. Some randomly selected MR images are depicted in Fig. 1. With regard to the time spent in the training process and in setting the training parameters, the network retrieval efficiency is improved. The back-propagation scheme is used to train the KNN-ANN. The final level of the KNN-ANN is tuned, keeping all other levels constant by freezing the weights. The first level in the KNN-ANN consists of the textural feature, and the upper levels consist of the domain's spatial features of the biomedical images. The training of the earlier levels can be quick, because of the textural features in this level. The upper levels are trained by fine-tuning to learn the MR image spatial features. The KNN-ANN framework presented learned these features in a self-learning mode. The VGG19 is appropriate for feature presentation and detection of special content in the biomedical image database. The focus of this paper is on the retrieval on MR images. The findings of this paper certify that VGG19, with weighted features of texture and shape and with KNN-ANN learning, is the best technique in the biomedical datasets retrieval framework. High retrieval efficiency is achieved utilizing KNN-ANN, with 90% retrieval compared to 70% using Euclidean metric distance. In addition, good results are obtained by performing the KNN-ANN, to project the feature representations into two-dimensional space. Therefore, KNN-ANN is effective in memory usage because of dimensionality reduction. An advantage of feature vectors with low dimensionality is their utility for indexing methods, which enhances the retrieval performance for a large-scale database. The efficiency of the CBMIR relates to similarity measurement between the biomedical database and the query. For measuring feature similarity, Euclidean and cosine distances are utilized, but they are limited because of the semantic

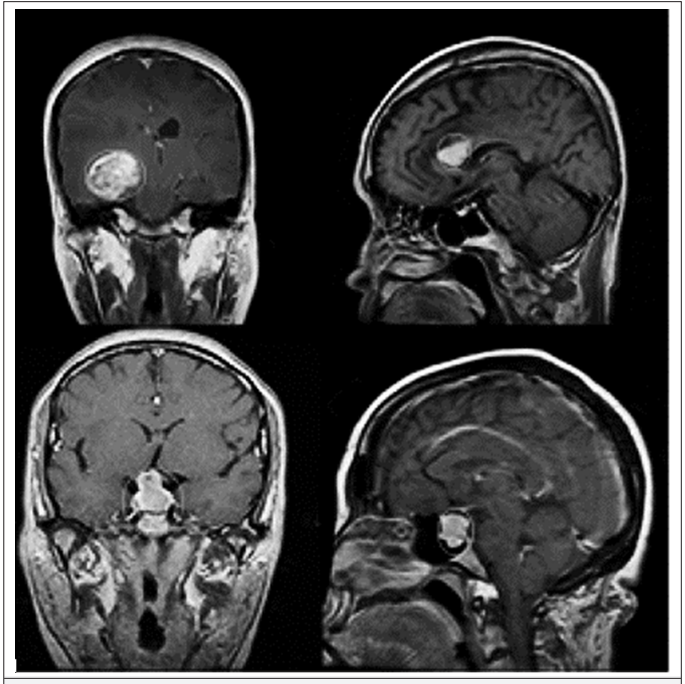

Fig. 1. Differing appearance of tumor in class 1and 2.

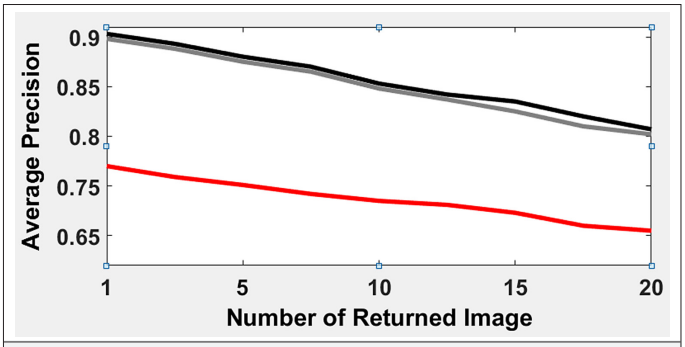

Fig. 2. Average precision of different methods for MRI database (black line: proposed method, gray line: ref [9], Red line: ref [6]).

gap [11,12]. The squared Mahalanobis (SM) technique is utilized to specify the optimum measurement parameter, which extends class similarity. The SM technique is used in KNN and the obtained results

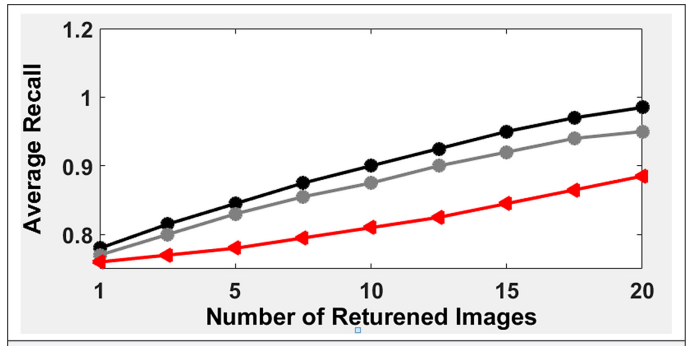

Fig. 3. Different methods comparison for average recall of CBMIR systems (black line: proposed method, gray line: ref [9] Red line: ref [6]).

TABLE II. AVERAGE RECALL PERCENTAGE COMPARISON, THE PRESENTED CBMIR SYSTEMS FOR 20 IMAGES OF MR IMAGE DATASET

	KNN-ANN+Shape	KNN-ANN+RADON	KNN-ANN+ Combined Feature
Class 1	60%	76%	90%
Class 2	65%	71%	95%
Class 3	66%	77%	94%

TABLE III. CORRECT IMAGE NUMBER RETRIEVAL FOR DIFFERENT PRESENTED SCHOLARS (20 RANDOM QUERIES)

	Ref. [6]	Ref. [9]	KNN-ANN+Combined Feature
Class 1	16	16	**20**
Class 2	15	15	**20**
Class 3	18	17	**19**

are significant. The MR image database accidentally divided the images into five sets, the same as [1-4], with no overlap of the various kinds of brain tumors; and the MR images from the identical patients were not simultaneously used in both the testing and the training sets. The first set is utilized as the test database, and the others are utilized as the training databases. Each MR image in the test database

TABLE I. CORRECTED RETRIEVAL NUMBER FOR MR IMAGES RETURNED FROM BIOMEDICAL IMAGE DATASET IN FIVE DIFFERENT TESTS IN THREE CLASSES

Class1			Class2			Class3		
KNN-ANN+ Combined Feature	KNN-ANN+ RADON	KNN-ANN+ Shape	KNN-ANN+ Combined Feature	KNN-ANN+RADON	KNN-ANN+ Shape	KNN-ANN+ Combined Feature	KNN-ANN+ RADON	KNN-ANN+ Shape
10	9	5	10	7	6	10	9	6
10	9	6	10	8	5	9	8	7
10	10	7	10	10	6	9	8	6
10	9	6	10	9	7	10	9	5
10	9	7	9	8	6	10	8	6

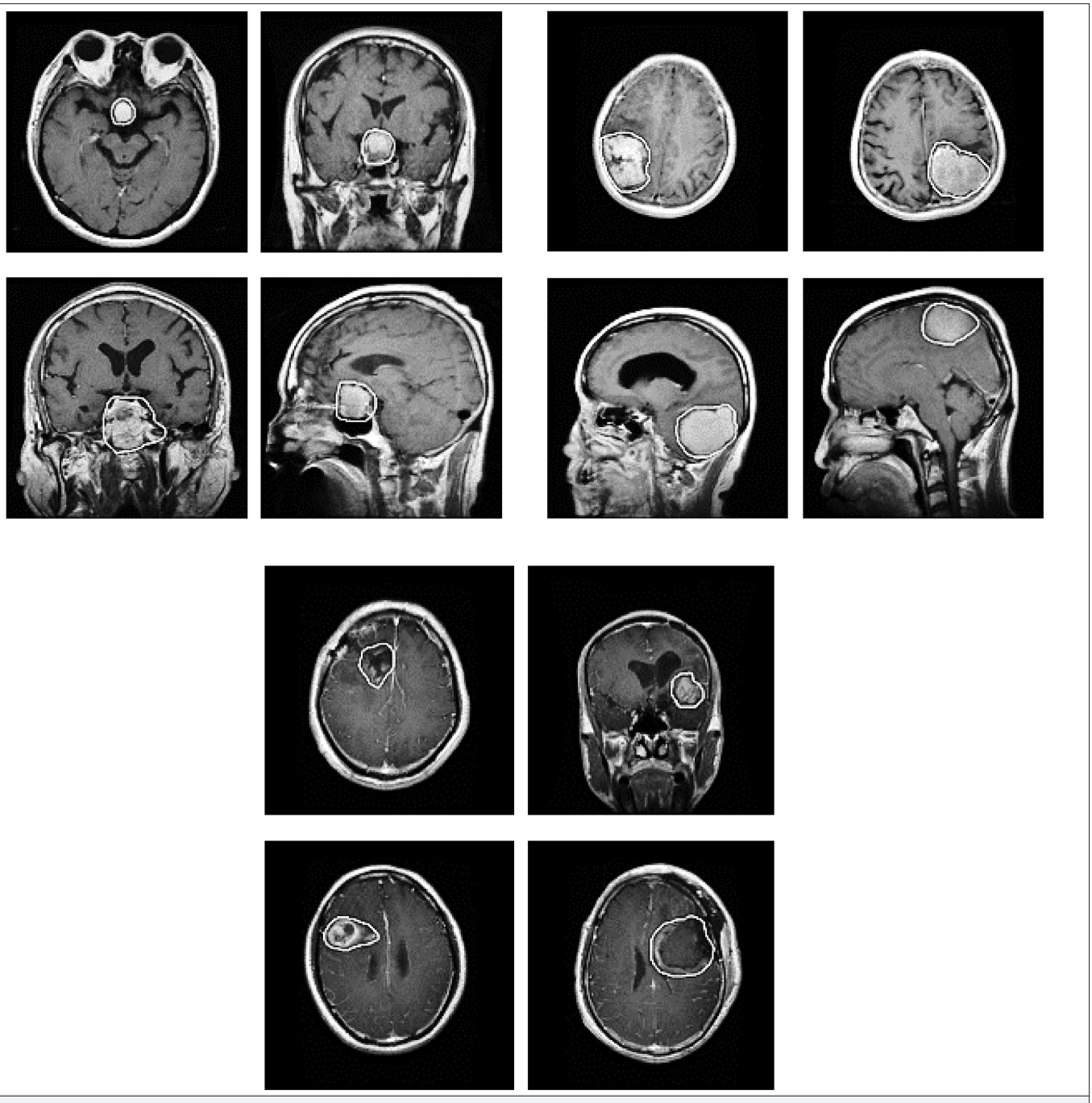

Fig. 4. MR image retrieval for presented CBMIR systems for query image.

(first database) attends the query. The mean value of accuracy is the routine parameter for accuracy computation percentage. This percentage illustrates that the images belong to the defined class. The system efficiency when rating the presented system is illustrated at Table III. As Table III depicts, the old methods are less accurate. The presented system achieves 90% retrieval for all the classes, and the other systems [6,9] have a lower rate of success. The proposed system has better performance In comparison with [6] and [9]. This system uses the weighting approach in which high-level features, besides the VGG features for large data sets, are tuned with an engineering view. In addition, KNN-ANN plays a major role in achieving the higher percentage of retrieval. Fig. 2 & Fig. 3 depict the average p-recision & average recall of the retrieval for the different numbers of MR images. The findings certify that the system is more efficient than other systems for large biomedical MR images. Table 1, Tables II and III and Fig. 4 depict that the system performance when using KNN-ANN with weighted features is the best choice for medical systems. It can be a smart assistant for MR image medical operators.

Database #2: This database comprises MRI images, consisting of 9000 images in three categories, each category containing 3000 MRI images. The MR image databases at (www.figshare.com/articles/bra

in_tumor_dataset/1512427) are used. The images have been widely used for CBMIR research. The database covers three classes of tumors. The standard for calculating the retrieval accuracy is the average precision:

$$p\ (i) = \frac{1}{100} \sum_{r(i,j)\le 100,\ 1\le j\le 100\ ID(j)=ID(i)} 1 \tag{13}$$

ID(*i*) is image *i* category numbers, *ID*(*j*) is image *j* category numbers, *p*(*i*) is the query image *i*, and average precision.

r(*i*, *j*) is the image *j* rank. *r* (*i*, *j*) illustrates the images and the percentage belonging to the image *i* category in the first-retrieved database images.

For the category *t,* the average precision is:

$$p_t(i) = \frac{1}{100} \sum_{1\le j\le 100,\ ID(i)=t} 1 \tag{14}$$

For database 2, average retrieval and recall are shown in Fig. 5 and 6 with comparison of different methods. It is clear that the presented system has better performance in comparison with the studies conducted by previous scholars [6] and [9] in database 2. We understood that the proposed method's retrieval accuracy is much better than the system of [6]. Table IV demonstrates the average retrieval accuracy for the both databases when the transform features have been utilized in the studied system. In Table IV, the performance of the proposed technique with standard wavelet (SW), shift invariant complex wavelet (SICW), and Gabor are compared. It is clear from Table IV that the retrieval accuracy of the R-transform is higher than that of the mentioned transform. The retrieval accuracy of different techniques in which both shape and texture features are utilized is demonstrated in Table V. We understood that the proposed system has better performance than the previous studies conducted by scholars in [6] and [14-16]. It is clear that when the number of retrieved images increases, the retrieval precision increases.

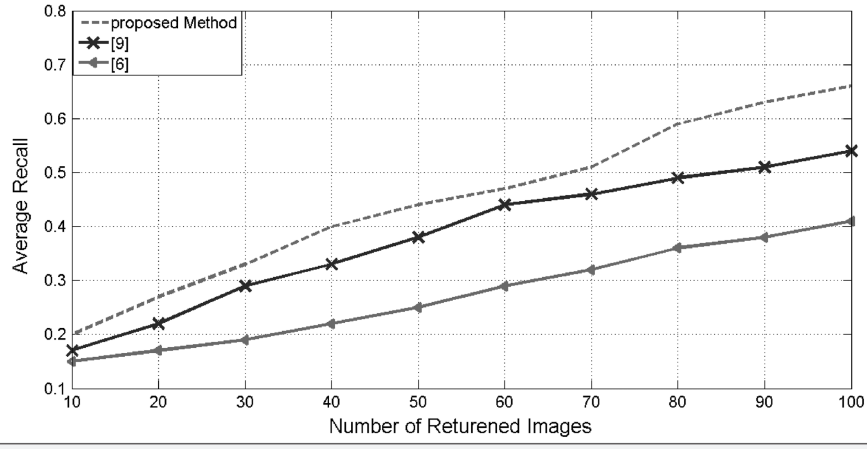

Fig. 5. Precision for database 2 in comparison of different methods.

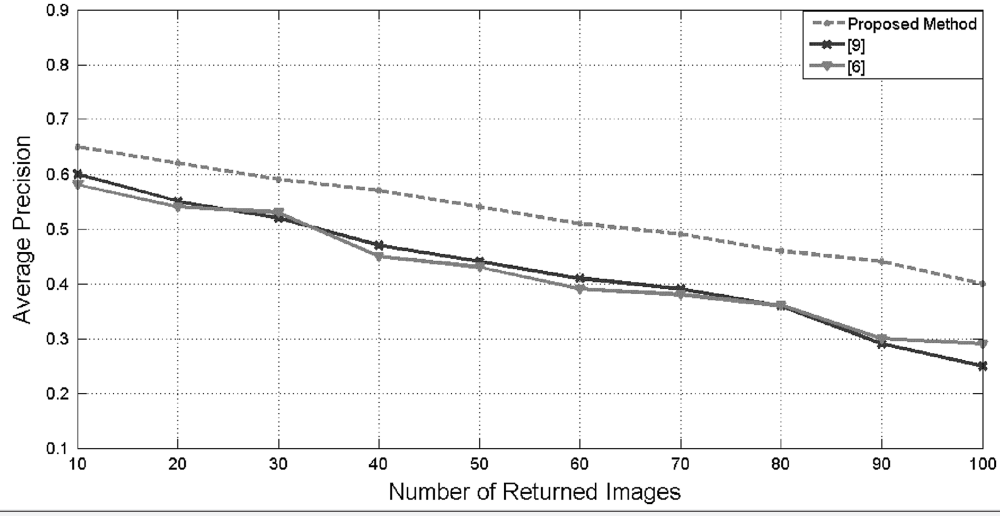

Fig. 6. Recall for database 2 in comparison of different methods.

TABLE IV. DATABASES 1 AND 2: RETRIEVAL ACCURACY WHEN TRANSFORMED FEATURES ARE UTILIZED

	Gabor [3]	Wavelets [4]	Shift Invariant Complex Wavelet [5]	Proposed Method
Database 1	73%	70%	77%	**88%**
Database 2	43%	40%	56%	**79%**

V. SHIFT INVARIANT AND ROTATION SPECIFICATION OF R-TRANSFORM

For database 1, experiments are done in order to certify that R-transform is rotation and shift invariant. The following steps demonstrate the rotation invariance characteristic:

- Step 1: Image rotation by the chosen values of different degrees.
- Step 2: Feature generation of each specific rotation, utilizing R- transform.
- Step 3: Calculation of the variance and energy in each rotation evaluated on each class of images.
- Step 4: σ and E comparison, calculated in the previous step.

It is shown in Table V that the average parameters of σ and E for rotations are approximately equal. We can deduce that R-transform is invariant against rotation.

The MSPE standard is utilized in order to check shift invariance specification. It is calculated as the error between the features of the original image and the circularly rotated image:

$$MSPE = \frac{1}{K}\sum_{t=1}^{K}\frac{\|A_t - F_t\|}{\|A_t\|} \quad (15)$$

A_t is features before shift and F_t is features after shift.

K is feature vector length. The maximum shift is equal to K.

TABLE V. ROTATION INVARIANCE PROPERTY OF R-TRANSFORM

	Rotation	E	σ
Class 1	0°	0.75	1.03
	30°	0.78	1.02
	60°	0.77	1.02
	90°	0.76	1.02
Class 2	0°	1.00	2.25
	30°	0.97	2.29
	60°	0.89	2.22
	90°	0.99	2.20
Class 3	0°	0.55	1.75
	30°	0.44	1.73
	60°	0.51	1.66
	90°	0.47	1.85

Lower values of MSPE show that the R-transform is more invariant to shift. Shift of 15 is used in this study. Table VI shows the MSPE for the orientations of 40° (shown by MSPE1) and 65° (denoted as MSPE2). It is observed from Table VI that R-transform is shift invariant. Table VII shows comparison of the recall percentage of the proposed system and the other previous retrieval systems when different numbers of images are retrieved (databases 1 and 2). Table VIII shows feature vector length and feature extraction time of different methods for a query image in database 2. Both Tables VII and VIII guarantee that the aforementioned system is the best one in feature vector length and retrieval process.

VI. CONCLUSION

An outstanding framework for integrated matching between the query and the database was presented for image similarity check which decreased the complexity by one-third. The R-transform was calculated and the variance and energy of the different degrees were utilized as the textural features. Besides, the invariant Hu moments of the edge biomedical image were utilized to introduce robust shape features. The experiments studied on double databases show the effectiveness of the proposed system compared to the previous studies. The new system achieves more than 90% retrieval. The feature vector dimension in our proposed algorithm is less than the other techniques. In addition, the time for processing and the complexity of calculation are less than the previous proposed systems,

TABLE VI. SHIFT INVARIANCE SPECIFICATION OF DIFFERENT TRANSFORMS FOR DIFFERENT MSPE

	Shift Invariance Property	MSPE1	MSPE2
R-transform		0.001	0.003

TABLE VII. RECALL PERCENTAGE COMPARISON OF THE PROPOSED SYSTEM AND THE DIFFERENT RETRIEVAL SYSTEMS WHEN DIFFERENT NUMBERS OF IMAGES ARE RETRIEVED

	2	5	10	20	30
[14]	62	68	83	86	88
[15]	70	79	84	87	90
[16]	90	93	95	96	97
Proposed Method database 1	**93**	**95**	**96**	**97**	**98**
Proposed Method database 2	**90**	**94**	**94**	**97**	**97**

TABLE VIII. FEATURE EXTRACTION TIME AND FEATURE VECTOR LENGTH IN DATABASE 2 FOR A QUERY IN COMPARISON WITH DIFFERENT SYSTEMS

	[14]	[15]	[16]	Proposed Method
Feature vector length	400	Variable from 500 to larger lengths	Variable from 600 to larger lengths	**<220**
Feature generation time (s)	~1	1~3	~4	**<1**

which is a privilege in our CBMIR. The novel system for the retrieval of MR image database is presented based on KNN-ANN and combined features with VGG. For each MR image, average and standard deviation of the improved R-transform and the modified Hu moments are computed. Weighting features with VGG generates a robust feature for retrieval of biomedical MR images. For image similarity process, an alternative method for training the KNN-ANN is introduced. It shows the transferability of learning to the MR images database. The results illustrate that the new method has good value in retrieval and efficiency, in appraisement with other proposed CBMIR systems. The presented CBMIR needs an MR image as a query image to retrieve the appropriate tumor MR images from the biomedical database. The authors of this research declare that the presented CBMIR plays an outstanding role in MR image database retrieval.

Peer-review: Externally peer-reviewed.

Author Contributions: Concept – S.S., H.V., T.S., A.C.; Design – S.S., H.V., T.S., A.C.; Supervision – S.S., H.V., T.S., A.C.; Resources – S.S., H.V., T.S., A.C.; Materials – S.S., H.V., T.S., A.C.; Data Collection and/or Processing – S.S., H.V., T.S., A.C.; Analysis and/or Interpretation –S.S., H.V., T.S., A.C.; Literature Search – S.S., H.V., T.S., A.C.; Writing Manuscript – S.S., H.V., T.S., A.C.; Critical Review –S.S., H.V., T.S., A.C.

Declaration of Interests: The authors have no conflicts of interest to declare.

Funding: The authors declared that this study has received no financial support.

REFERENCES

1. M. Fakheri, T. Sedghi, M. G. Shayesteh, and M. C. Chehel Amirani, "Framework for image retrieval using machine learning and statistical similarity matching techniques," *IET Image Process.*, vol. 7, no. 1, pp. 1–11, Feb. 2013.
2. G. Takacs, V. Chandrasekhar, S. S. Tsai, D. Chen, R.Grzeszczuk, and B.Girod, "Fast computation of rotation-invariant image features by an approximate radial gradient transform," *IEEE Trans. Image Process.*, vol. 22, no. 8, pp.2970–2982, Apr. 2013.
3. G. Shan, W. Minghua, W. Lei, and Y. Cihui, "Reduced quaternion matrix for color texture classification," *Neural Comput. Appl.*, vol. 25, no. 3, pp. 945–954, Jun. 2014.
4. S. P. Chen, "W.single-shot imaging without reference wave using binary intensity pattern for optically-secured-based correlation," *IEEE Photonics J.*, vol. 8, no. 1, pp. 8–13, Aug. 2016.
5. S. Medina, and I. Biomed, "Normalization and Query Abstraction Based on SNOMED-CT and HL7: Supporting Multicentric Clinical Trials," *IEEE J. Biomed. Health. Inform.*, vol. 19, pp. 10–16, Jul. 2014.
6. T. Sedghi, "A fast and effective model for cyclic analysis and its application in classification," *Arab. J. Sci. Eng.*, vol. 38, no. 4, pp. 927–935, Sep. 2013.
7. P. Wu, S. C. H. Hoi, P. Zhao, C. Miao, and Z.-Y. Liu, "Onlinemulti-modal distance metric learning with application to imageretrieval," *IEEE Trans. Knowl. Data Eng.*, vol. 28, no. 2, pp. 454–467, Feb. 2016.
8. H. C. Shin *et al.*, "Deep convolutional neural networks for computer-aideddetection CNN architectures, dataset characteristics and transfer learning," *IEEE Trans. Med. Imag.*, vol. 35, no. 5, pp. 1285–1298, May. 2016.
9. S.Shafei, H.Vahdati, T. Sedghi, and A. Charmin, "Novel high level retrieval system based on mathematic algorithm & technique for MRI medical imaging and classification," *J. Instrum.*, vol. 16, no. 7, pp. 1–14, Jul. 2021.
10. J. Li, J. Wang, and J. Z. Wiederhold, "Integrated region matching for image retrieval in proceedings," *The 8th ACM International Conference on Multimedia*, pp. 147–156, Oct, 2015.
11. F. Baig *et al.*, "Boosting the Performance of the BoVW Model Using SURF–CoHOG-Based Sparse Features with Relevance Feedback for CBIR" *Iran. J. Sci. Technol. Trans. Electr. Eng.*, vol. 44, no. 1, pp. 99–118, Aug 2020.
12. M. h.Hajigholam, A. A.Raie, and K. Faez, "Using sparse representation classifier (SRC) to calculate dynamic coefficients for multitask joint spatial pyramid Matching, " *Iran. J. Sci. Technol. Trans. Electr. Eng.*, vol. 45, no. 1, pp. 295–307, 2021.
13. F.Rahdari, E.Rashedi, and M.Eftekhari, " A multimodal emotion recognition system using facial landmark analysis," *Iran. J. Sci. Technol. Trans. Electr. Eng.*, vol. 43, no. S1, pp. 171–189, Sep. 2019.
14. N. Hor, and S. Fekri-Ershad, "Image retrieval approach based on local texture information derived from predefined patterns and spatial domain information," *Int. J. Comput. Sci. Eng.*, vol. 8, no. 6, pp. 246–254, Dec 2019.
15. K. M. Hosny, R. M. Farouk, A. M. Alzohairy, and G. Hassan, "Efficient quaternion moments for representation and retrieval of biomedical color images," *Biomed. Eng. Appl. Basis Commun.*, vol. 32, pp. 1–16, Oct. 2020.
16. G. Hassan, K. M. Hosny, R. M. Farouk, and A. M. Alzohairy, "An efficient retrieval system for biomedical images based on Radial Associated Laguerre Moments," *IEEE Access*, vol. 8, pp. 175669–175687, Sep. 2020.

Shahin Shafei was born in Mahabad, Iran, in 1987. He received the B.S degree in electrical engineering from IAU Urmia, Urmia, Iran, in 2006. He received the M.S degree in electrical engineering in IAU Ahar, Iran, in 2009, and he graduated as a PHD student in electrical engineering in IAU Ahar, Iran. His research interests include image sensing, image fusion, intelligent computing and watermarking. He has published 14 papers in highly referred international journals.

Hamid Vahdati was born in Birjand city, in 1961. He received the B.S. degree in electrical engineering from the University of Sharif, Iran,in 1992 He received an M.S. degree in electrical engineering from Amirkabir University of Technology, Iran, in 1997 and Ph.D degree in electrical engineering from Amirkabir University of Technology, Iran, in 2008 .his main interest is in the area of signal processing.

Tohid Sedghi received his BS degree in electronic engineering from the Department of Electrical Engineering, Islamic Azad University, Urmia Branch, Urmia, Iran, in 2007. He received his MS degree in electrical engineering from the University of Urmia, Iran, in 2009. He got his PhD degree from the Department of Electrical Engineering, Science and Research Branch, Islamic Azad University, Tehran, Iran, in 2015. His research interests include antennas and propagation, radar application, intelligent computing, and data compression. He has published more than 30 papers in his referred international journal and more than 15 papers in national/international conferences. Now he is an assistant professor at the Department of Electrical Engineering, Islamic Azad University, Urmia Branch.

Asghar Charmin was born in Azarshahr city, East Azerbaijan Province, in 1974. He received the B.S. degree in electronic engineering from the University of Tabriz, Iran, in 1998, and an M.S. degree in electronic engineering from Amirkabir university of technology, Iran in 2000 and Ph.D degree in electronic engineering from Sahand University of Technology, Iran in 2017. his main interest being low-power, Delta-Sigma modulation-based converters.. Since 2001, he has been an Instructor at Islamic Azad University.